JOURNAL OF ENVIRONMENTAL SCIENCES 155 (2025) 613–621

Available online at www.sciencedirect.com

ScienceDirect

www.elsevier.com/locate/jes

JES JOURNAL OF ENVIRONMENTAL SCIENCES

www.jesc.ac.cn

Research Article

Boosting dimethyl carbonate synthesis from CO_2 and methanol through oxygen vacancy engineering on CeO_2 under thermodynamically favorable conditions

Yongcheng Xiao[1,**], *Bo Lei*[1,**], *Haoyang Jiang*[1], *Yi Xie*[1], *Junjie Du*[3], *Weigao Xu*[4], *Dekun Ma*[2,*], *Miao Zhong*[1,*]

[1] *College of Engineering and Applied Sciences, Collaborative Innovation Center of Advanced Microstructures, National Laboratory of Solid State Microstructures, the Frontiers Science Center for Critical Earth Material Cycling, Nanjing University, Nanjing 210023, China*

[2] *Zhejiang Key Laboratory of Alternative Technologies for Fine Chemicals Process, Shaoxing University, Shaoxing 312000, China*

[3] *Hefei National Research Center for Physical Sciences at the Microscale, Key Laboratory of Strongly-Coupled Quantum Matter Physics of Chinese Academy of Sciences, Key Laboratory of Surface and Interface Chemistry and Energy Catalysis of Anhui Higher Education Institutes, Department of Chemical Physics, University of Science and Technology of China, Hefei 230026, China*

[4] *Key Laboratory of Mesoscopic Chemistry, School of Chemistry and Chemical Engineering, Nanjing University, Nanjing 210023, China*

ARTICLE INFO

Article history:
Received 29 March 2024
Revised 27 May 2024
Accepted 27 May 2024
Available online 6 June 2024

Keywords:
Dimethyl carbonate synthesis
CO_2 activation
Oxygen vacancy cluster
Thermodynamic equilibrium
Catalytic activity

ABSTRACT

The direct conversion of greenhouse gas CO_2 and low-cost CH_3OH into valuable dimethyl carbonate (DMC) offers a promising low-carbon synthetic pathway, but the slow CO_2 activation kinetics and entropy-decreasing nature of this reaction significantly restrict DMC yield to below 1 %. In this work, 2-cyanopyridine (2-CP) was employed as a dehydrating agent to suppress the reverse reaction between DMC and H_2O, shifting the thermodynamic equilibrium in favor of DMC production. Under this thermodynamic unconstrained condition, increasing oxygen vacancies, especially in the form of oxygen vacancy clusters, promotes catalytic activity significantly. We achieve a catalytic activity of 211 mmol/(g·h) at 140 °C on H_2-treated, oxygen-vacancy-clusters-rich CeO_2 in the presence of 2-CP, a 1.6-fold increase compared to the activity with air-treated CeO_2 under identical conditions. The DMC yield reaches 8.54 % in a 20 mL CH_3OH solution with 2-CP, surpassing the calculated DMC yield of about 0.66 % from the reaction equilibrium constant under the same conditions and without using the dehydrating agent. This work suggests the importance of using a dehydrating agent and also highlights oxygen vacancy clusters as pivotal active sites to promote DMC

* Corresponding authors.
E-mails: dkma@usx.edu.cn (D. Ma), miaozhong@nju.edu.cn (M. Zhong).
** These authors contributed equally to this work.

https://doi.org/10.1016/j.jes.2024.05.048

synthesis. Achieving sustainable DMC synthesis requires further exploration, encompassing strategies such as methods for regeneration of 2-CP.

Introduction

Dimethyl carbonate (DMC) possesses non-corrosive and biodegradable properties, making it highly valuable for various applications, such as used as a polar solvent, fuel additive, and battery electrolyte (Árvai and Mika, 2023; Cai et al., 2010; Li et al., 2021; Wang et al., 2022). The global industry demonstrates a substantial demand for DMC, with its projected market value exceeding $1.2 billion by 2025 (Li et al., 2023; Shao et al., 2023; Zhang et al., 2023). The conventional techniques employed for the synthesis of DMC include urea alcoholysis method, transesterification method, phosgene method, and oxidative carbonylation method. However, these approaches involve the main challenges of the high raw material price, the use of toxic reagents and the production of waste CO_2 emissions. Therefore, the search for a low-cost and environmentally friendly method for DMC synthesis is crucial. The direct synthesis of DMC using heterogeneous catalysts from waste CO_2 and cost-effective CH_3OH opens up a more environmentally friendly and sustainable alternative (Zhang et al., 2021; Zhong et al., 2020). Despite the promising prospects of this DMC synthesis pathway, it still encounters substantial challenges due to the thermodynamic constraints and difficulties in activating CO_2 at low temperatures below 200 °C.

In recent years, the catalysts for DMC synthesis from CO_2 and CH_3OH have made significant progress, with the emergence of both homogeneous and heterogeneous catalysts (Zhang et al., 2021). Homogeneous catalysts, including ionic liquid and alkaline carbonate catalysts, face challenges such as poor stability and separation difficulties. In contrast, heterogeneous catalysis using transition metal oxides, heteropoly acids, and metal catalysts have gained attention for their high stability and easy product separation. Among the heterogeneous catalysts, CeO_2-based materials have emerged as one of the most efficient catalysts for DMC synthesis from CH_3OH and CO_2 (Shi et al., 2022). This is attributed to the presence of abundant oxygen vacancies (V_O) on CeO_2 surfaces, serving as active sites for CO_2 activation through the modulation of the C=O bond angle and bond length of adsorbed CO_2 (Zhang et al., 2019). Studies have indicated that the CeO_2 (110) surface, in particular, exhibits a lower formation energy for V_O compared to (100) and (111) facets, making it ideal for DMC synthesis (Marciniak et al., 2020; Zhang et al., 2017). Doping CeO_2 with foreign elements has also been shown to increase the density of V_O for enhanced activity. For example, Liu's group demonstrated a DMC activity of 7.1 mmol/(g·h) over Zr-doped CeO_2 nanorods (Liu et al., 2018). In addition, H_2 treatment can increase V_O density, Fu's group showed CeO_2 nanowire treated in H_2 with a catalytic activity of 3.4 mmol/(g·h) (Fu et al., 2018). Further exploration revealed that the V_O clusters (which contain more than two V_O) exhibit higher activity than isolated V_O (Huang et al., 2020).

Despite progress in understanding the role of V_O in CeO_2 for improving DMC synthesis, these insights have primarily been derived from the reactions under the conditions significantly constrained by the reaction thermodynamics at extremely low reaction rates ranging from 1 to 20 mmol/(g·h) and a low overall DMC yield of < 1 %, even with the most current active CeO_2 catalyst (O'Neill et al., 2022; Xuan et al., 2019). Hence, it remains uncertain whether the established correlations between the catalytic activity and the electronic properties and structures of active sites, along with doping modifications, accurately reflect the catalysts' efficacy under high reaction rates free from thermodynamic constraints. This includes the conditions involving adding dehydrating agents capable of modulating thermodynamic equilibrium of DMC synthesis. In the previous studies, Honda and Tomishige used 2-cyanopyridine (2-CP) as a dehydrating agent to enhance the catalytic activity of DMC synthesis on CeO_2, resulting in a high DMC yield of 94 % using a small amount of 100 mmol CH_3OH and 50 mmol 2-CP after 12 h reaction (Honda et al., 2013). Extensive research on DMC synthesis underscores that the use of CeO_2 as catalyst and 2-CP as a dehydrating agent yields high DMC yields. Studies have also delved into the impact of doping and H_2-treatment on CeO_2 for DMC synthesis without dehydrating agents, however, the synergy between 2-CP usage and CeO_2 modifications needs further exploration (Kuan et al., 2023; Wang et al., 2015; Zhang et al., 2023).

In this study, we investigated DMC synthesis from CO_2 and CH_3OH using a variety of CeO_2-based catalysts in the presence of 2-CP. We observed that the hydrothermally synthesized CeO_2 nanorods with the predominantly exposed (110) facet exhibited higher activity than metal-doped CeO_2 nanorods, showing a reaction rate of 135 mmol/(g·h) for DMC synthesis with 2-CP. Further annealing CeO_2 nanorods in a 5 % H_2 atmosphere (H_2-treated CeO_2) increased the density of V_O clusters. The V_O-clusters-rich H_2-treated CeO_2 showed a reaction rate of 211 mmol/(g·h), a 1.6-fold increase compared to pristine CeO_2 under identical conditions. The DMC yield reached 8.54 % at 140 °C, which suggests that 2-CP and V_O clusters improve the catalytic activity of the reaction.

1. Experimental

1.1. *Catalyst preparation*

Preparation of CeO_2 catalysts: Typically, 5 mmol $CeCl_3{\cdot}7H_2O$ were dissolved into 10 mL deionized water (DI) to prepare the precursor solution. The solution was then added dropwise into a 60 mL solution of 10 mol/L NaOH. After 10 min of magnetic stirring, the solution was transferred to a 100 mL autoclave and hydrothermally treated at 120 °C for 24 h. After the hydrothermal treatment, the products were collected by centrifugation and washed with DI water several times,

and then dried in a glass tube under a low vacuum condition (pumped by a mechanical oil diffusion pump) at room temperature. The as-prepared catalysts were calcined at 450 °C for 4 h in atmospheres of O_2, air, Ar, and 5 % H_2 (H_2: Ar = 5:95, vol./vol.), respectively, and the obtained products were denoted as O_2-treated CeO_2, Air-treated CeO_2, Ar-treated CeO_2 and H_2-treated CeO_2, respectively.

Preparation of metal-doped CeO_2-based solid solution catalysts: The metal-doped CeO_2 catalysts were synthesized via co-precipitation of cerium salt and another metal salt, followed by hydrothermal treatment and annealing. Accordingly, a precursor solution containing cerium salt and another metal salt was prepared by uniformly mixing 4.5 mmol of $CeCl_3{\cdot}7H_2O$ and 0.5 mmol of the metal salt in 10 mL of DI water. After 10 min of magnetic stirring, the solution was carefully transferred to a 100 mL autoclave and subjected to hydrothermal treatment at 120 °C for 24 h. Following the hydrothermal treatment, the resulting products were collected through centrifugation and subsequently washed multiple times with deionized (DI) water. Finally, the products were dried in a glass tube under a low vacuum condition, utilizing a mechanical oil diffusion pump, at room temperature. The as-synthesized catalysts were calcined at 450 °C for 4 h in an atmosphere of 5 % H_2 (H_2: Ar = 5:95, vol./vol.). The obtained catalysts were denoted as $Ce_{0.9}M_{0.1}O_2$, where M represents the corresponding doped metal element (i.e., In, Zr…).

1.2. *Characterization*

Transmission electron microscope (TEM) were used to obtain morphology images (Tecn F20 instrument, Netherlands). Scanning electron microscope (SEM) images were captured with a Hitachi Regulus SU8100 instrument (Japan). X-ray diffraction patterns (XRD) were acquired using a Bruker Advantage D8 diffractometer with Cu (Kα) radiation (Germany), and the detection angle of 2θ was scanned from 10° to 80° X-ray photoelectron spectroscopy (XPS) analysis was performed using a PHI5000 VersaProbe instrument (Japan). Raman spectra were recorded by a microspectrophotometer (Horiba-LabRAM HR, France) with a 532 nm laser as the excitation source. The positron annihilation lifetime measurement was carried out on a fast-fast coincidence lifetime spectrometer (TechnoAP/DPAMS-LCA, Japan) at an ambient temperature. The positron source (^{22}Na) was sandwiched between the two identical samples for measurement. Each measurement was performed for 4 h to reach two million counts. The lifetime components were resolved by using a life time 9.0 program. The ASAP-2460 analysis system (USA) at 77 K (Micromeritics) were employed to obtain N_2 adsorption–desorption isotherms. Brunauer-Emmett-Teller (BET) model were used to calculated the specific surface areas of all the samples.

1.3. *Catalytic performance evaluation*

The DMC synthesis reaction was carried out in a 100 mL autoclave reactor. Typically, in the case where the 2-CP dehydrating agent was not used, 0.1 g catalysts and 20 mL CH_3OH were added into the autoclave reactor. When employing the dehydrating agent, 0.05 g catalysts, 20 mL CH_3OH, and 4 g 2-CP were added into the autoclave reactor. Before the reaction, the autoclave reactor was purged with 1 MPa CO_2 several times. Subsequently, the autoclave reactor was pressurized up to 2.5 MPa, heated to 140 °C, and kept for 2 h. After the reaction, the products were analyzed by the gas chromatograph with a flame ion detector (FID-GC, KB-FFAP) using 1-propanol ($CH_3CH_2CH_2OH$) as an internal standard substance. After the reaction, 1 mL of reaction solution was mixed with 0.5 mL of 1-propanol, and approximately 4 μL of the resulting mixture was introduced into FID-GC for product detection.

2. Results and discussion

As shown in Fig. 1, the synthesis of DMC using green CH_3OH and waster CO_2 offers a promising solution to reducing carbon footprint and fostering sustainable chemical production.

Fig. 1 – Eco-friendly synthesis route of DMC utilizes green CH_3OH and greenhouse gas CO_2.

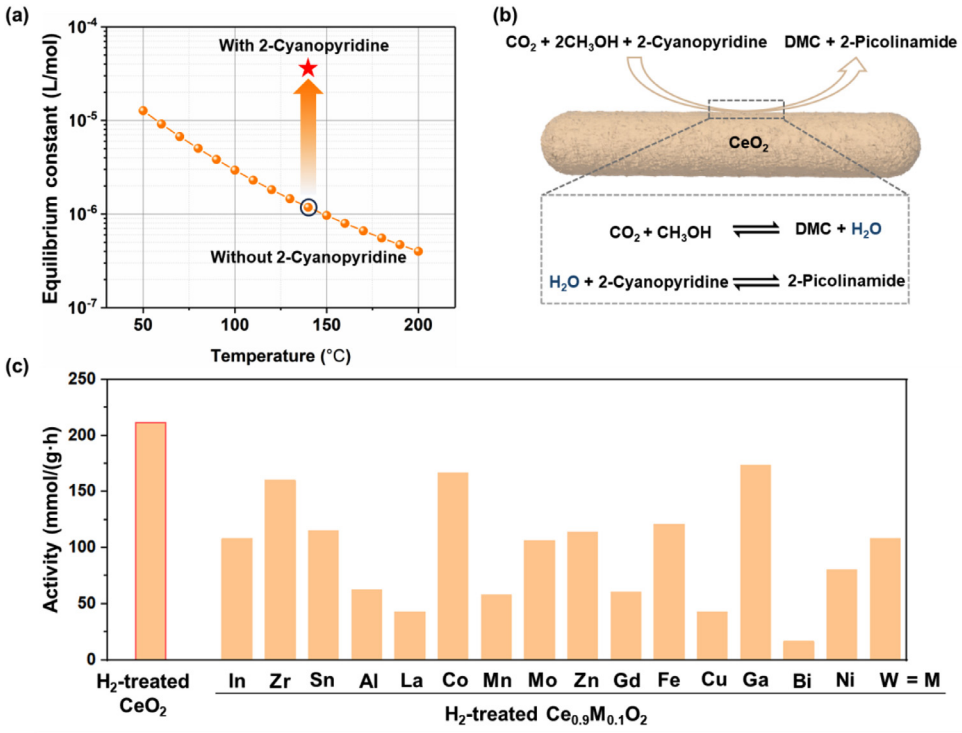

Fig. 2 – (a) The calculated equilibrium constants for DMC synthesis from CO_2 and CH_3OH as a function of the reaction temperature without 2-CP, and the orange arrow indicates the increasing 2-CP production with the presence of 2-CP for in situ removal of generated H_2O; (b) a schematic representation of DMC synthesis on CeO_2 with 2-CP; (c) catalytic performance for DMC synthesis on different H_2-treated CeO_2 and metal-doped CeO_2 with 2-CP. According to the ratios of metal atoms added into the precursor solution during the hydrothermal synthesis, the metal-dopant concentrations were 10 % in all cases. All catalysts were annealed in a 5 % H_2 atmosphere at 450 °C for 4 h.

This process presents significant advancement in the utilization of CO_2 for high-value synthesis. In an ideal scenario, CO_2 could be captured directly from the atmosphere, while CH_3OH production could be achieved via CO_2 hydrogenation using renewable H_2 derived from clean sources such as solar and wind energy (Feng et al., 2023; Sutherland, 2019). Despite its promise, the synthesis of DMC from CH_3OH and CO_2 still faces challenges pertaining to reaction thermodynamics and catalytic activity. These obstacles underscore the need for further research and development to optimize reaction conditions and enhance catalytic activity, thus realizing the full potential of this environmentally friendly synthetic route.

As shown in Fig. 2a, the equilibrium constants for DMC synthesis from CO_2 and CH_3OH under conventional conditions, without using dehydrating agents, were calculated using the thermodynamic parameters listed in Appendix A Table S2. The detailed calculations are provided in the Appendix A Supplementary data. At the reaction temperature of 80–180 °C, the equilibrium constants for this reaction are notably small, ranging from 10^{-5} to 10^{-7}, indicating a preference for the reverse reaction. Assessing the catalytic activity potential for catalysts becomes challenging due to the stringent thermodynamic restrictions. Modifying the reaction equilibrium presents a viable strategy to address these constrains. An effective approach involves the removal of the product H_2O by adding a dehydrating agent such as 2-CP (Bansode and Urakawa, 2014; Honda et al., 2013). After the introduction of the dehydrating agent 2-CP, the of generated H_2O was in situ removed from catalyst surfaces, thus shifting the reaction equilibrium in favor of DMC synthesis as indicated with the orange arrow in Fig. 2a. The reaction between 2-CP and H_2O, yielding 2-PA, allows for in situ consumption of H_2O, thereby boosting DMC synthesis (Fig. 2b). Under such conditions, CeO_2-based catalysts exhibited remarkable activity for DMC synthesis from CO_2 and CH_3OH. Further studies delved into the doping effect in CeO_2 for DMC synthesis. Various metal elements were doped into CeO_2, and their catalytic activities for DMC synthesis in the presence of 2-CP were examined. Appendix A Fig. S1 illustrates the XRD patterns of the CeO_2 and the metal-doped CeO_2 catalysts, indicating a uniform fluorite structure without phase separation. Fig. 2c shows that, under thermodynamically favorable conditions, H_2-treated CeO_2 exhibits superior catalytic activity compared to the other metal-doped CeO_2 in a 10 at.% metal doping level.

The SEM images in Fig. 3a and Appendix A Fig. S2–S4 depict the morphology of the CeO_2 catalysts synthesized via a hydrothermal method and atmospheric annealing. The nanorods showed an average length of 0.5–1 μm, contrasting with the commercial CeO_2 which exhibited a bulky cuboid shape morphology. Fig. 3b and c illustrate the high-resolution (HR)-TEM images and corresponding fast Fourier transform (FFT) analysis results of H_2-treated CeO_2. The HR-TEM analysis

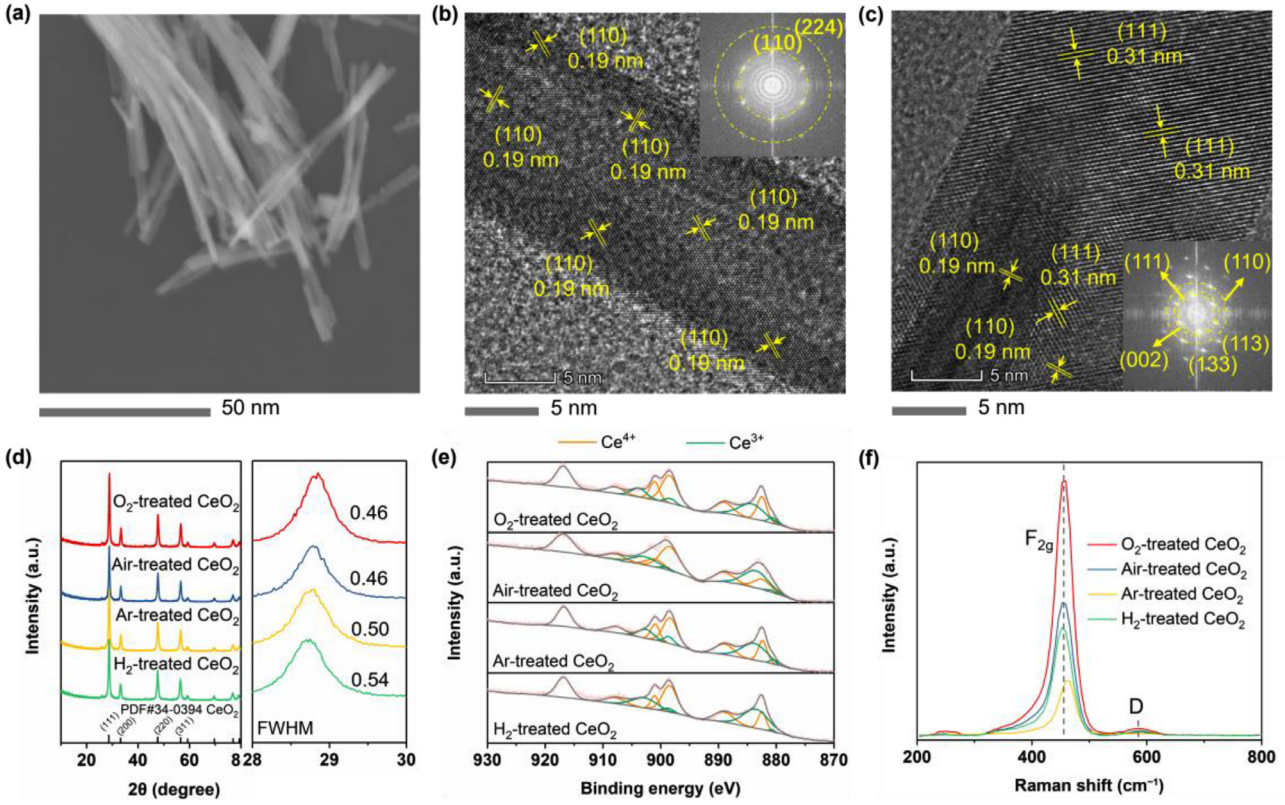

Fig. 3 – (a) SEM image of H_2-treated CeO_2; (b) and (c) HR-TEM images of H_2-treated CeO_2 and the corresponding fast Fourier transform analyses data; (d–f) XRD patterns, XPS spectra, and Raman spectra of the CeO_2 nanorods treated with different annealing conditions.

Table 1 – The grain sizes, specific surface areas (S_{BET}), and Ce^{3+} ratios of different CeO_2 catalysts.

Sample	O_2-treated CeO_2	Air-treated CeO_2	Ar-treated CeO_2	H_2-treated CeO_2
Grain size (nm)	17.6	17.6	16.2	15.0
S_{BET} (m^2/g)	51.2	49.6	54.2	57.6
Ce^{3+}	28.7 %	31.9 %	33.8 %	37.8 %

revealed crystallographic features of H_2-treated CeO_2, with d-spacings of 0.19, 0.27, and 0.31 nm, corresponding to the (110), (001), and (111) facets of CeO_2. Although the FFT analysis results indicated the presence of high-index crystal facets, such as (224), (113), and (133), (110) was a predominantly exposed crystal facet on CeO_2 nanorods. Fig. 3d displays the XRD patterns of CeO_2 catalysts, wherein the diffraction peaks at 28.7°, 33.2°, 47.6°, and 56.5° were attributed to the (111), (200), (220), and (311) crystal facets of fluorite structure CeO_2 (PDF#34–0394), consistent with the TEM images. As listed in Table 1, the grain size of CeO_2 catalysts was 15–18 nm calculated using the Debye-Scherrer formula ($D = \frac{k\lambda}{B\cos\theta}$) ($D$ (nm) is grain size; k is Scherrer's constant; λ is X-ray wavelength; B is full width at half maximum (FWHM); θ (°) is diffraction angle), and the data for the values of FWHM of the (111) crystal facet were provided in Fig. 3d. The smaller grain size may indicate a larger V_O concentration (Trogadas et al., 2012). The nitrogen adsorption–desorption isotherms of CeO_2 catalysts are shown in Appendix A Fig. S6, demonstrating the type-H3 hysteresis loops (Kuan et al., 2022). As listed in Table 1, the Brunauer–Emmett–Teller specific surface areas (S_{BET}) of O_2-treated CeO_2, Air-treated CeO_2, Ar-treated CeO_2, and H_2-treated CeO_2 were calculated to be 51.2, 49.6, 54.2, and 57.6 m^2/g, respectively, showing a small variation in specific surface areas. Fig. 3e presents the XPS fine spectra of Ce 3d for the CeO_2 catalysts. The Ce 3d spectra were fitted with ten peaks, denoted as u^0 (~ 898.6 eV), u (~ 901.0 eV), u′ (~ 902.8 eV), u″ (~ 907.8 eV), and u‴ (~ 916.8 eV) peaks and v^0 (~ 880.7 eV), v (~ 882.4 eV), v′ (~ 883.5 eV), v″ (~ 889.0 eV) and v‴ (~ 898.4 eV) peaks, representing the spin-orbit splitting of Ce $3d_{3/2}$ and Ce $3d_{5/2}$ orbitals, respectively (Jiang et al., 2023). The ratio of Ce^{3+} related to V_O could be determined by calculating the ratio of the areas of the u^0, u', v^0, and v' peaks to the total peak area. As a result, the Ce^{3+} ratios of O_2-treated CeO_2, Air-treated CeO_2, Ar-treated CeO_2, and H_2-treated CeO_2 were 28.7 %, 31.9 %, 33.8 %, and 37.8 %, respectively. Since the proportion of Ce^{3+} is an important indicator of V_O numbers, these results illustrate that the annealing atmosphere can regulate the density of V_O in CeO_2

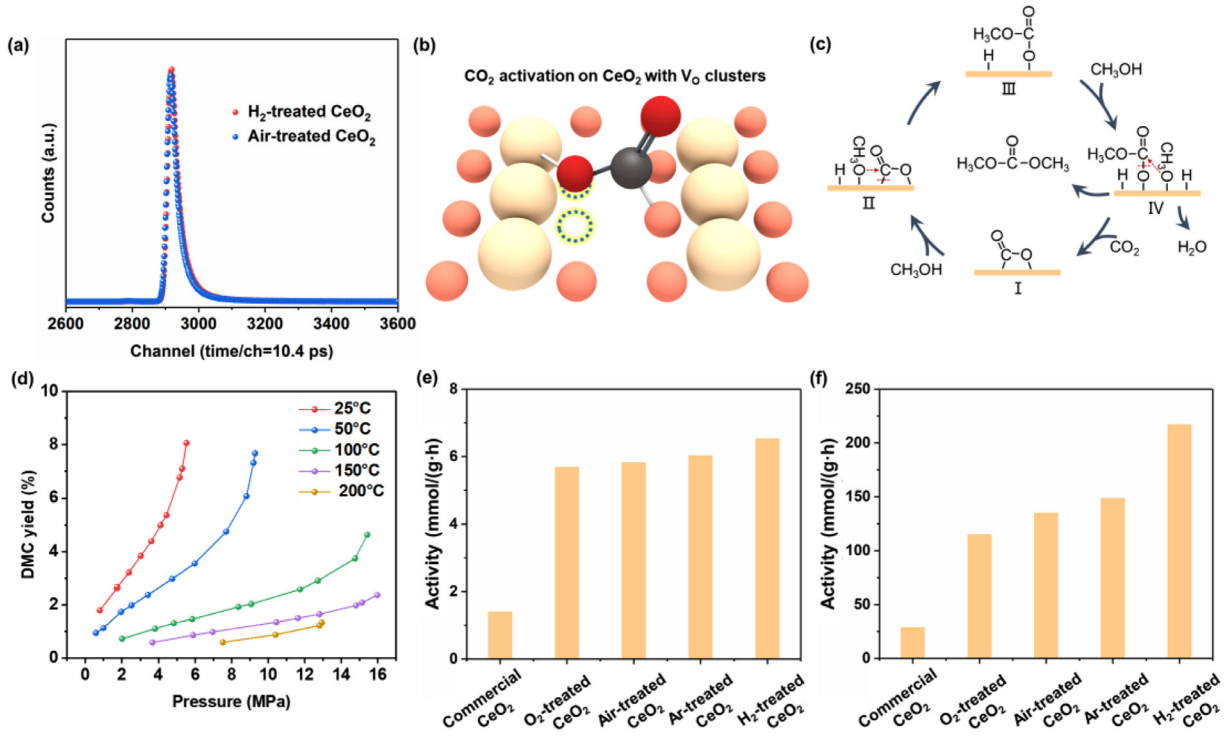

Fig. 4 – (a) Positron annihilation lifetime spectra; (b) schematic illustration of CO_2 activation in V_O clusters; (c) possible reaction mechanism for DMC synthesis from CO_2 and CH_3OH; (d) the calculated DMC yield at various temperatures and pressures; (e) catalytic performance of different CeO_2 catalysts without 2-CP; (f) catalytic performance of different CeO_2 catalysts with 2-CP.

catalysts, with a reducing atmosphere during annealing facilitating the formation of V_O. Fig. 3f displays the Raman spectra, revealing a peak at 456.9 cm^{-1} attributed to the symmetrical stretching of Ce—O F_{2g} mode, and the peak at 590.1 cm^{-1} assigned to defect-induced (D) mode associated with Ce^{3+} in the lattice, which is induced by V_O (Gong et al., 2020; Kulal et al., 2023). HR-TEM images indicated that H_2-treated CeO_2 has a predominantly exposed (110) facet. The obvious D peaks of CeO_2 catalysts in Raman implied the formation of oxygen vacancies on CeO_2 catalysts. Furthermore, the results of XPS suggested that H_2-treated CeO_2 has the most Ce^{3+} compared with other CeO_2 catalysts, indicating H_2-treated CeO_2 has the most of V_O.

The positron annihilation technique exhibits exceptional sensitivity towards atomic-scale defects, allowing for the distinction of various types of V_O (oxygen vacancy) (Liu et al., 2009). We employed this technology to investigate the types and relative intensities of V_O in the CeO_2 catalysts annealed under different atmospheric conditions. The positron annihilation lifetime spectra of the CeO_2 catalysts consisted of three distinct lifetime components, denoted as τ_1, τ_2, and τ_3, with corresponding relative intensities denoted as I_1, I_2, and I_3, respectively (Wang et al., 2017). The shortest lifetime component τ_1 represents small neutral Ce^{3+}–V_O associates (isolated V_O), the slightly longer lifetime component τ_2 represents V_O clusters (V_O aggregates), and the longest lifetime component τ_3 represents large voids within CeO_2 (Liu et al., 2009). Positron annihilation lifetime spectra and the spectral data are shown in Fig. 4a and Table 2, respectively. From the data in the table, it can be observed that H_2-treated CeO_2 exhibited a higher relative intensity of V_O clusters compared with Air-treated CeO_2, reaching a value of 30.8 %. This indicated that the reducing atmosphere promoted the formation of V_O clusters. Additionally, the longer τ_2 lifetime of H_2-treated CeO_2 than Air-treated CeO_2 suggested the presence of higher abundance of V_O associated in the former (Han et al., 2023). As shown in Fig. 4b, V_O clusters on the surface of CeO_2 facilitate the activation of CO_2, and possible reaction mechanism for DMC synthesis from CO_2 and CH_3OH are proposed in Fig. 4c (Daniel et al., 2023; Kuan et al., 2022). The calculated equilibrium DMC yield provided a more intuitive demonstration of the severe thermodynamic constraints on this reaction. Due to the reaction taking place in a liquid-phase environment, we established the relationship between temperature, CO_2 pressure, and CO_2 solubility in CH_3OH to calculate the reaction equilibrium, as shown in Fig. 4d and Appendix A Table S3 (O'Neill et al., 2022). When the reaction temperature exceeds 100 °C, the equilibrium yield of DMC does not surpass 1 %, even under significantly high pressures of CO_2. As shown in Fig. 4e, in the absence of 2-CP, the DMC synthesis reaction faced severe thermodynamic constraints, resulting in lower apparent catalytic activity. Additionally, there was minimal difference in catalytic activity among the different atmosphere annealing CeO_2 catalysts. H_2-treated CeO_2 showed the best catalytic activity of 6.5 mmol/(g·h), Air-treated CeO_2 exhibited a lower catalytic activity of 5.8 mmol/(g·h), and they were both much better than commercial CeO_2 of 1.4 mmol/(g·h). To improve the activity, the dehydrating 2-CP was introduced to in situ re-

Table 2 – The data of positron annihilation lifetime spectra.

Sample	τ_1 (ps)	I_1	τ_2 (ps)	I_2	τ_3 (ps)	I_3
H_2-treated CeO_2	154.6 ± 0.0	65.5 % ± 0.9 %	386.9 ± 0.0	30.8 % ± 0.9 %	1984.0 ± 22.0	3.8 % ± 0.1 %
Air-treated CeO_2	154.2 ± 0.0	71.5 % ± 0.7 %	385.1 ± 0.0	24.2 % ± 0.8 %	1975.0 ± 21.0	4.8 % ± 0.1 %

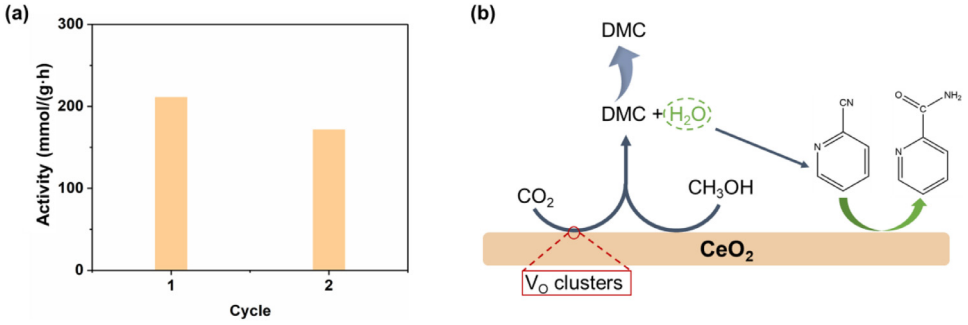

Fig. 5 – (a) Cycling stability for H_2-treated CeO_2, (b) reaction mechanism on CeO_2 catalysts for DMC synthesis reaction with 2-CP.

move H_2O generated during the reaction. As depicted in Fig. 4f, the addition of 2-CP resulted in a substantial increase in catalytic activity. Notably, the catalytic activity of H_2-treated CeO_2 reached 211 mmol/(g·h), which is superior to the results of the literature report (Appendix A Table S5). In the presence of 2-CP, small amounts of methyl carbamate and methyl picolinate maybe generated as by-products in addition to the main products DMC and 2-PA (Bansode and Urakawa, 2014; Honda et al., 2013). H_2-treated CeO_2 exhibited a high DMC yield of 8.54 % when using 2-CP, surpassing the calculated equilibrium DMC yield of about 0.66 % without using the dehydrating agent. In addition, the difference in catalytic activity with CeO_2 treated in different gas atmospheres was consistent with the variations in V_O cluster concentrations in the corresponding samples. With the increase in V_O cluster concentrations in the CeO_2 nanorods, the activity for DMC synthesis became more pronounced.

As obtained, the addition of 2-CP effectively modulated the equilibrium toward DMC synthesis. Following the first round of DMC synthesis at 140 °C for 2 h, the catalytic activity decreased in the second reaction cycle, primarily due to the instability of CeO_2 under this reaction conditions with 2-CP (Fig. 5a) (Stoian et al., 2018). As shown in Appendix A Fig. S7, XPS analysis was conducted on the post-reaction H_2-treated CeO_2. The results indicated an extra N 1 s peak appeared in the post-reaction H_2-treated CeO_2, which is attributed to the adsorption of 2-PA on the CeO_2 surface (Stoian et al., 2018). Such adsorption of 2-PA may lead to the poisoning of surface active sites, consequently reducing catalytic activity. Further efforts are expected to increase the stability of CeO_2 in 2-CP during the reaction and explore ways to effectively regenerate 2-CP for sustainable DMC synthesis. The C=O bond in CO_2 possesses a bond energy as high as 806 kJ/mol, making it challenging to activate, especially at low temperatures of 80–180 °C (Jiang et al., 2023). However, efficient activation of CO_2 is necessary for the rate-determining step ($CH_3OCOO^* \rightarrow CH_3OCO^* + O^*$) in DMC synthesis (Li et al., 2022). V_O clusters can enhance the activation of CO_2 on CeO_2 surface, thereby promoting the synthesis of DMC. Finally, in light of the previous report (Honda et al., 2014), we proposed a similar reaction pathway for the synthesis of DMC from CH_3OH and CO_2 on CeO_2 catalysts with the presence of 2-CP, as shown in Fig. 5b. Specifically, with the insertion of methoxy to adsorbed CO_2, dimethyl carbonate (DMC) is formed. On CeO_2, the by-product H_2O reacts with 2-CP to produce 2-PA, promoting DMC production (Daniel et al., 2023; Kuan et al., 2022; Tian et al., 2023).

3. Conclusions

In summary, we have explored the influence of oxygen vacancy density and types on catalytic activity for dimethyl carbonate (DMC) synthesis under thermodynamically unconstrained conditions. The introduction of a dehydrating agent (2-CP) significantly enhances catalytic activity by in situ consuming by-product H_2O. While doping various metals into CeO_2 shows a minor impact on DMC synthesis under thermodynamic unconstrained condition, boosting oxygen vacancies, particularly in the form of oxygen vacancy clusters, proves beneficial for catalytic activity. Annealing CeO_2 in a reducing H_2 atmosphere (H_2-treated CeO_2) shows a high catalytic activity of 211 mmol/(g·h) for DMC synthesis. This study demonstrates that oxygen vacancy clusters can effectively promote CO_2 activation and enhance DMC synthesis. Also, thermodynamically favorable conditions assist in understanding the relations between active sites and their activities. This study further suggests that methods for regenerating the dehydrating agent, such as 2-CP, are urgently needed for sustainable DMC synthesis. In addition, the value of adding 2-CP for DMC synthesis should be further considered in the future

research, including the cost of 2-CP and the cost of product separation, which are vital factors to determine its economically viability.

Declaration of competing interest

The authors declare that they have no known competing financial interests or personal relationships that could have appeared to influence the work reported in this paper.

CRediT authorship contribution statement

Yongcheng Xiao: Writing – original draft, Investigation, Conceptualization. **Bo Lei:** Writing – original draft, Investigation. **Haoyang Jiang:** Writing – original draft, Validation. **Yi Xie:** Validation. **Junjie Du:** Validation, Conceptualization. **Weigao Xu:** Investigation. **Dekun Ma:** Writing – review & editing, Software, Formal analysis. **Miao Zhong:** Writing – review & editing, Validation, Supervision, Conceptualization.

Acknowledgments

This work was supported by the National Natural Science Foundation of China (Nos. 22272078 and 52371196), the National Key Research and Development Program of the Ministry of Science and Technology of China (No. 2020YFA0406102), and the "Innovation and Entrepreneurship of Talents plan" of Jiangsu Province.

Appendix A Supplementary data

Supplementary material associated with this article can be found in the online version at doi:10.1016/j.jes.2024.05.048.

References

Árvai, C., Mika, L.T., 2023. Recent advances in catalytic carbonylation reactions in alternative reaction media. Chin. J. Chem. 42, 406–429.

Bansode, A., Urakawa, A., 2014. Continuous DMC synthesis from CO_2 and methanol over a CeO_2 catalyst in a fixed bed reactor in the presence of a dehydrating agent. ACS Catal. 4, 3877–3880.

Cai, Q.H., Zhang, L., Shan, Y.K., He, M.Y., 2010. Promotion of ionic liquid to dimethyl carbonate synthesis from methanol and carbon dioxide. Chin. J. Chem. 22, 422–424.

Daniel, C., Farrusseng, D., Schuurman, Y., 2023. Investigating the reaction mechanism of dimethyl carbonate synthesis through isotopic labeling experiments. Catal. Commun. 179, 106697.

Feng, Z., Tang, C., Zhang, P., Li, K., Li, G., Wang, J., et al., 2023. Asymmetric sites on the $ZnZrO_x$ catalyst for promoting formate formation and transformation in CO_2 hydrogenation. J. Am. Chem. Soc. 145, 12663–12672.

Fu, Z., Yu, Y., Li, Z., Han, D., Wang, S., Xiao, M., et al., 2018. Surface reduced CeO_2 nanowires for direct conversion of CO_2 and methanol to dimethyl carbonate: catalytic performance and role of oxygen vacancy. Catalysts 8, 164.

Gong, Z.-J., Li, Y.-R., Wu, H.-L., Lin, S.D., Yu, W.-Y., 2020. Direct copolymerization of carbon dioxide and 1,4-butanediol enhanced by ceria nanorod catalyst. Appl. Catal. B 265, 118524.

Han, T., Cao, X., Chen, H.-C., Ma, J., Yu, Y., Li, Y., et al., 2023. Photosynthesis of benzonitriles on BiOBr nanosheets promoted by vacancy associates. Angew. Chem. Int. Ed. 62, e202313325.

Honda, M., Tamura, M., Nakagawa, Y., Nakao, K., Suzuki, K., Tomishige, K., 2014. Organic carbonate synthesis from CO_2 and alcohol over CeO_2 with 2-cyanopyridine: scope and mechanistic studies. J. Catal. 318, 95–107.

Honda, M., Tamura, M., Nakagawa, Y., Sonehara, S., Suzuki, K., Fujimoto, K., et al., 2013. Ceria-catalyzed conversion of carbon dioxide into dimethyl carbonate with 2-cyanopyridine. ChemSusChem 6, 1341–1344.

Huang, Z.-Q., Li, T.-H., Yang, B., Chang, C.-R., 2020. Role of surface frustrated Lewis pairs on reduced CeO_2(110) in direct conversion of syngas. Chinese J. Catal. 41, 1906–1915.

Jiang, H., Wang, L., Kaneko, H., Gu, R., Su, G., Li, L., et al., 2023. Light-driven CO_2 methanation over Au-grafted $Ce_{0.95}Ru_{0.05}O_2$ solid-solution catalysts with activities approaching the thermodynamic limit. Nat. Catal. 6, 519–530.

Kuan, W.-F., Chung, C.-H., Lin, M.M., Tu, F.-Y., Chen, Y.-H., Yu, W.-Y., 2023. Activation of carbon dioxide with surface oxygen vacancy of ceria catalyst: an insight from in-situ X-ray absorption near edge structure analysis. Mater. Today Sustainab. 23, 100425.

Kuan, W.-F., Yu, W.-Y., Tu, F.-Y., Chung, C.-H., Chang, Y.-C., Lin, M.M., et al., 2022. Facile reflux preparation of defective mesoporous ceria nanorod with superior catalytic activity for direct carbon dioxide conversion into dimethyl carbonate. Chem. Eng. J. 430, 132941.

Kulal, N., Bhat, S.S., Hugar, V., Mallannavar, C.N., Lee, S.-C., Bhattacharjee, S., et al., 2023. Integrated DFT and experimental study on Co_3O_4/CeO_2 catalyst for direct synthesis of dimethyl carbonate from CO_2. J. CO_2 Util. 67, 102323.

Li, L., Liu, W., Chen, R., Shang, S., Zhang, X., Wang, H., et al., 2022. Atom-economical synthesis of dimethyl carbonate from CO_2: engineering reactive frustrated Lewis pairs on ceria with vacancy clusters. Angew. Chem. Int. Ed. 61, e202214490.

Li, L., Liu, Z., Yu, X., Zhong, M., 2023. Achieving high single-pass carbon conversion efficiencies in durable CO_2 electroreduction in strong acids via electrode structure engineering. Angew. Chem. Int. Ed. 62, e202300226.

Li, L., Ozden, A., Guo, S., Garcıá de Arquer, F.P., Wang, C., Zhang, M., et al., 2021. Stable, active CO_2 reduction to formate via redox-modulated stabilization of active sites. Nat. Commun. 12, 5223.

Liu, B., Li, C., Zhang, G., Yao, X., Chuang, S.S.C., Li, Z., 2018. Oxygen vacancy promoting dimethyl carbonate synthesis from CO_2 and methanol over Zr-Doped CeO_2 nanorods. ACS Catal. 8, 10446–10456.

Liu, X., Zhou, K., Wang, L., Wang, B., Li, Y., 2009. Oxygen vacancy clusters promoting reducibility and activity of ceria nanorods. J. Am. Chem. Soc. 131, 3140–3141.

Marciniak, A.A., Henrique, F.J.F.S., de Lima, A.F.F., Alves, O.C., Moreira, C.R., Appel, L.G., et al., 2020. What are the preferred CeO_2 exposed planes for the synthesis of dimethyl carbonate? Answers from theory and experiments. Mol. Catal. 493, 111053.

O'Neill, M.F., Sankar, M., Hintermair, U., 2022. Sustainable synthesis of dmethyl- and diethyl carbonate from CO_2 in batch and continuous flow-lessons from thermodynamics and the importance of catalyst stability. ACS Sustain. Chem. Eng. 10, 5243–5257.

Shao, W., Zhang, X., Xie, Y., 2023. Engineering active sites and recognizing mechanisms for CO_2 fixation to dimethyl carbonate. Trends Chem. 5, 312–323.

Shi, D., Heyte, S., Capron, M., Paul, S., 2022. Catalytic processes for the direct synthesis of dimethyl carbonate from CO_2 and methanol: a review. Green Chem. 24, 1067–1089.
Stoian, D., Medina, F., Urakawa, A., 2018. Improving the stability of CeO_2 catalyst by rare earth metal promotion and molecular insights in the dimethyl carbonate synthesis from CO_2 and methanol with 2-Cyanopyridine. ACS Catal. 8, 3181–3193.
Sutherland, B.R., 2019. Pricing CO_2 direct air capture. Joule 3, 1571–1573.
Tian, L., Tan, Z., Wang, Q., Liao, Y.-S., Chou, J.-P., Wu, J.-M., et al., 2023. Cerium coordination-dependent surface intermediates regulate activity in dimethyl carbonate synthesis from CO_2 and methanol. Appl. Catal. B 336, 122914.
Trogadas, P., Parrondo, J., Ramani, V., 2012. CeO_2 surface oxygen vacancy concentration governs in situ free radical scavenging efficacy in polymer electrolytes. ACS Appl. Mater. Interfaces 4, 5098–5102.
Wang, L., Yu, Y., He, H., Zhang, Y., Qin, X., Wang, B., 2017. Oxygen vacancy clusters essential for the catalytic activity of CeO_2 nanocubes for o-xylene oxidation. Sci. Rep. 7, 12845.
Wang, M., Luo, L., Wang, C., Du, J., Li, H., Zeng, J., 2022. Heterogeneous catalysts toward CO_2 hydrogenation for sustainable carbon cycle. Acc. Chem. Res. 3, 565–571.
Wang, S.-P., Zhou, J.-J., Zhao, S.-Y., Zhao, Y.-J., Ma, X.-B., 2015. Enhancements of dimethyl carbonate synthesis from methanol and carbon dioxide: the in situ hydrolysis of 2-cyanopyridine and crystal face effect of ceria. Chin. Chem. Lett. 26, 1096–1100.
Xuan, K., Pu, Y., Li, F., Luo, J., Zhao, N., Xiao, F., 2019. Metal-organic frameworks MOF-808-X as highly efficient catalysts for direct synthesis of dimethyl carbonate from CO_2 and methanol. Chinese J. Catal. 40, 553–566.
Zhang, G., Zhou, Y., Yang, Y., Kong, T., Song, Y., Zhang, S., et al., 2023. Elucidating the role of surface Ce^{4+} and oxygen vacancies of CeO_2 in the direct synthesis of dimethyl carbonate from CO_2 and methanol. Molecules 28, 3785.
Zhang, M., Xu, Y., Williams, B.L., Xiao, M., Wang, S., Han, D., et al., 2021. Catalytic materials for direct synthesis of dimethyl carbonate (DMC) from CO_2. J. Clean. Prod. 279, 123344.
Zhang, S., Huang, Z.-Q., Ma, Y., Gao, W., Li, J., Cao, F., et al., 2017. Solid frustrated-Lewis-pair catalysts constructed by regulations on surface defects of porous nanorods of CeO_2. Nat. Commun. 8, 15266.
Zhang, S., Xia, Z., Zou, Y., Cao, F., Liu, Y., Ma, Y., et al., 2019. Interfacial frustrated Lewis pairs of CeO_2 activate CO_2 for selective tandem transformation of olefins and CO_2 into cyclic carbonates. J. Am. Chem. Soc. 141, 11353–11357.
Zhong, M., Tran, K., Min, Y., Wang, C., Wang, Z., Dinh, C.-T., et al., 2020. Accelerated discovery of CO_2 electrocatalysts using active machine learning. Nature 581, 178–183.